Structural impact resilience of lightweight fiber-reinforced LECA concrete using ANN and RSM technique

Idris Ahmed Ja'e [a,b,*], Zakaria Che Muda [c], Hamad Almujibah [d], Chiemela Victor Amaechi [a,e,*], Agusril Syamsir [a], U. Johnson Alengaram [f], Ali.E.A. Elshekh [d], Maaz Osman Bashir [d]

[a] Institute of Energy Infrastructure, Universiti Tenaga Nasional, Putrajaya Campus, Jalan IKRAM-UNITEN, Kajang, Selangor 43000, Malaysia
[b] Department of Civil Engineering, Ahmadu Bello University, Zaria 810107, Nigeria
[c] Faculty of Engineering and Quantity Surveying, INTI-International University, Persiaran Perdana BBN Putra Nilai, Nilai 71800, Malaysia
[d] Department of Civil Engineering, College of Engineering, Taif University, P.O. Box 11099, Taif City 21974, Saudi Arabia
[e] Engineering Department, Lancaster University, Lancaster LA1 4YR, UK
[f] Department of Civil Engineering, Faculty of Engineering, University of Malaya, Kuala Lumpur 50603, Malaysia

ARTICLE INFO

ABSTRACT

The structural impact resilience of lightweight Lightweight Expanded Clay Aggregate (LECA) concrete refers to its capacity to withstand impact and other related loading effectively. Achieving a balance between lightweight properties and structural performance is crucial; however, research in this scope remains limited. This study explores these characteristics by evaluating the concrete's ability to absorb impact energy, crack resistance relative to compressive strength, and its residual life. The concrete mix incorporates polypropylene fibres (PPF) between 0 % and 3 %, and the natural aggregate is entirely replaced with LECA. Slab specimens of varying thicknesses were subjected to varying low-velocity impact loadings and the results at both service and ultimate state were analysed using ANN and RSM. Intricate relationships between the material's composition and its overall impact behaviour demonstrated a strong correlation with PPF below 1.0 % showing notable effects on workability, compressive, split tensile and flexural strengths while contributing to a density reduction. A general improvement in impact resilience parameters is observed in direct proportion to PPF and thickness – up to 33 times in impact energy absorption and up to 17 times in crack resistance. However, higher residual strength is exhibited in concrete with lower thickness due to its greater toughness, further highlighting a significant influence of the fibre-to-concrete dimension ratio on the impact resilience of the concrete. Moreso, results from both ANN and RSM demonstrated strong agreement in all responses within a 95 % confidence interval and R-square of 0.987.

1. Introduction

The utilisation of lightweight concrete in construction is an age-long practice, which can be traced back to 128 A.D. in ancient Rome. Specifically, exemplified by the construction of the dome of the Pantheon, spanning over 43 m [1]. Generally, foaming agents [2,3] or lightweight aggregates such as slate, shale, beads, lightweight expanded clay aggregates (LECA) and other synthetic aggregates [4–7] are incorporated to achieve an overall reduced concrete density of 1400 kg/m³ – 1840 kg/m³, compared to 2200 kg/m³ – 2400 kg/m³ for conventional concrete. The reduced density is a result of the porous medium created by either partially or completely incorporating lightweight aggregate instead of natural coarse aggregate [8,9]. Thus, offers several advantages in the construction of high-rise buildings, bridge decks, protective barriers etc, thereby making it cost-effective [10–13]. Detailed guidance on structural lightweight aggregate and general requirements can be found in ACI PRC-213 [14] and ASTM C331/C331M[15].

Unlike the natural aggregate, which can withstand 60–80 % of compressive loads, the LECA is capable of carrying only about 40 – 60 % compressive load. This limitation directly influences the concrete which

Table 1

Oxide composition of Cement and Micro-silica used.

Oxide component	Composition (%)	
	Cement	Micro-silica
Lime (CaO)	64.34	1.85
Silica (SiO$_2$)	21.48	92.9
Alumina (Al$_2$O$_3$)	5.60	0.16
Alkalies (K$_2$O, Na$_2$O)	0.44	1.04
Sulphur Trioxide (SO$_3$)	2.24	-
Magnesia (MgO)	2.07	0.26
Iron Oxide (Fe$_2$O$_3$)	2.26	0.58
TiO$_5$	0.51	-
P$_2$O$_5$	0.17	-
Loss of Ignition (LOI)	0.64	0.3

is known to have a direct relation with the impact energy absorption. Therefore, it is crucial to enhance the cement matrix and interfacial transition zone (ITZ) to improve LECA concrete performance. To maximize the load-bearing capacity, the concrete mix must focus on ensuring a robust ITZ. Additionally, the void spaces inherent in lightweight concrete facilitate energy dissipation, thereby reducing the likelihood of brittle failure due to their large deformation capability [16].

The Impact energy absorption of concrete refers to its ability to accommodate and dissipate a certain threshold of impact loading before the emanation of cracks. These characteristics are crucial for applications where concrete must withstand sudden forces, such as protective barriers, blast-resistant structures, and seismic-resistant structures. When subjected to impact loading, the energy is absorbed through different mechanisms, including deformation of the concrete matrix, followed by the crushing of aggregate and subsequent propagation of cracks that ultimately lead to failure [17]. Despite the several highlighted advantages of lightweight concrete, it also presents some drawbacks, such as reduced mechanical strength [18], longevity-related issues, and an early susceptibility to crack formation. For this reason, research efforts to overcome these challenges have been reported and related investigations are still ongoing [19,20–23,24,25,26,27]. For instance, a recent study explores the impact performance of a lightweight oil palm shell (OPS) concrete when subjected to impact loading under varying boundary conditions [28], considering up to 5 % polypropylene fibre and 8 boundary conditions. The findings demonstrated a remarkable enhancement, with impact energy absorption and crack resistance showing improvements of 20 and 29 times, respectively, compared to plain OPS concrete. Another study reported an impressive 80 % increase in flexural and impact energy absorption when basalt fibre was included in lightweight aggregate concrete [29]. The use of fibre in lightweight aggregate concretes has also been acknowledged to address issues such as low strength and impact toughness, even in harsh environments. Specifically, incorporating 6 kg/m3 of fibre has been
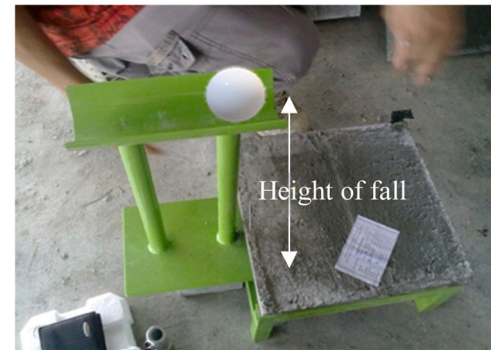
shown to mitigate strength loss under freeze-thaw cycles by effectively bearing tensile stress and preventing crack propagation [30]. Furthermore, the addition of 1.15 % hooked-end steel fibre in lightweight aggregate concrete resulted in a reported 20-fold improvement in fracture energy[31]. In this context, the present study employs the Artificial Neural Network (ANN) and Response Surface Methodology (RSM) to predict the energy absorptions and crack resistance of lightweight fibre-reinforced LECA concrete subjected to impact loading.

The recent trend of in integrating ML algorithms in research has yielded several benefits in modelling and predicting concrete
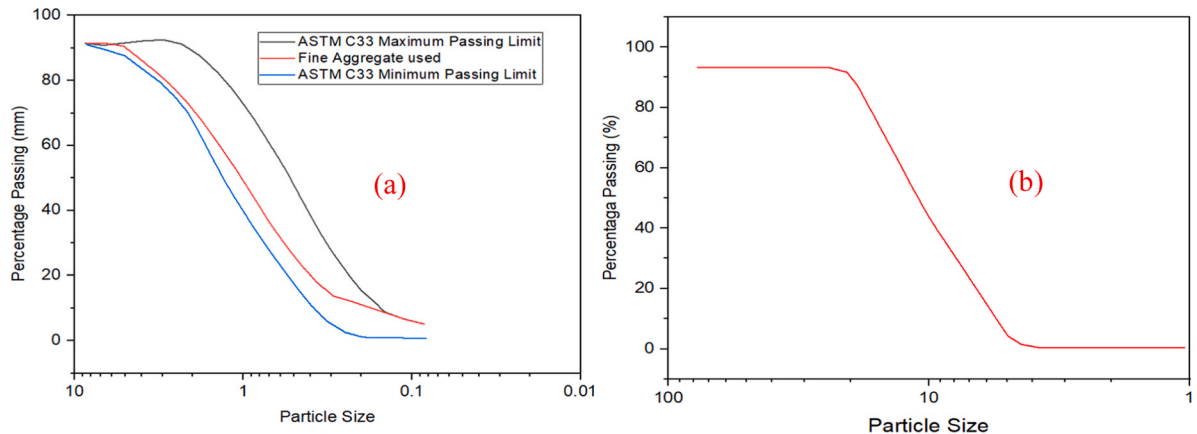
Table 2

PPF and slab thickness from experimental design.

Run	PPF (%)	Slab Thickness (mm)	Run	PPF (%)	Slab Thickness (mm)
1	0	30	19	0	50
2	0.75	30	20	0.75	50
3	1	30	21	1	50
4	1.5	30	22	1.5	50
5	1.75	30	23	1.75	50
6	2	30	24	2	50
7	2.5	30	25	2.5	50
8	2.75	30	26	2.75	50
9	3	30	27	3	50
10	0	40	28	0	60
11	0.75	40	29	0.75	60
12	1	40	30	1	60
13	1.5	40	31	1.5	60
14	1.75	40	32	1.75	60
15	2	40	33	2	60
16	2.5	40	34	2.5	60
17	2.75	40	35	2.75	60
18	3	40	36	3	60

Fig. 2. Low-velocity impact test set-up.

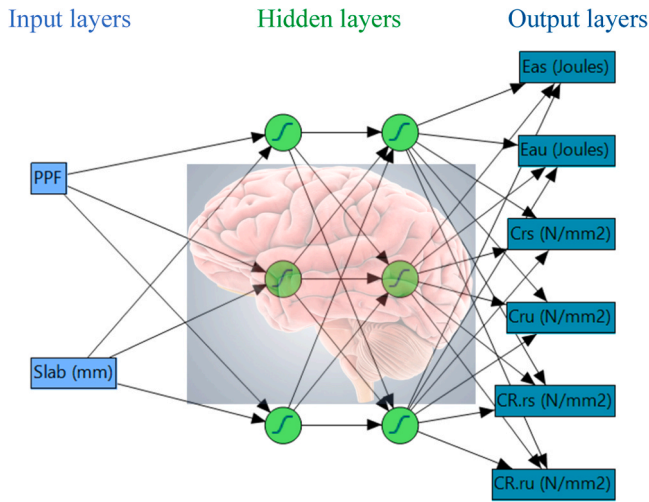**Fig. 1.** Particle size distributions (a) Fine Aggregate (b) LECA.

Fig. 3. Developed ANN model structure.

correlation of up to 0.97 with minimal error [37]. Lin and Wu[38] also predicted the compressive strength of concrete using ANN, leaveraging database of actual concrete mix proportions sourced from the literature. The ANN model adopted in the study has been shown to outperform the models in the referenced studies. Similarly, the predicted compressive strength of concrete produced from recycled aggregate using ANN and Response Surface Methodology (RSM) was investigated [39]. The findings indicated strong correlations between the ANN and RSM-predicted responses based on the statistical comparisons. Other studies utilised ANN to predict the mechanical properties of rubberised concrete subjected to elevated temperatures [40], while additional studies explored the compressive strength of concrete containing metakaolin [41], all have demonstrated strong correlations with the referenced experimental results.

Although previous studies have proposed models to predict the mechanical properties of different types of concrete [42]. There are limited studies focused on predicting the structural impact resilience of lightweight fibre-reinforced LECA concrete. Hence, this study aims to bridge this gap by utilising ANN and RSM to investigate the resilience of t LECA concrete under impact loading. The research will explore energy absorption, crack resistance, and residual strength across varying proportions of polypropylene fibre (PPF) and different concrete thicknesses. This is crucial because the impact performance influences other properties, including compressive strength and flexural behaviour. The LECA is considered a complete substitute for the natural aggregate. The test specimens consisted of 300 mm square slabs of varying thicknesses ranging between 30 mm to 60 mm, each containing PPF between 0 % and 3 %. Furthermore, a single dose of micro-silica has been added to the concrete mix to fill up the void spaces in the LECA and the ITZ, while

performance, particularly due to their ability to handle complex problems with high precision [32–35]. In addition, the utilisation of ML prediction models such as ANN comes with many advantages in terms of reduced cost, economical material utilisation, and time. Several studies have employed ANN to predict different concrete responses and more. For instance, Maqsoom et al.[36] combined ANN with multivariate regression to predict concrete properties cured in hot weather. Another study integrated ANN with SVM to predict the type of fly ash concrete, with the models demonstrating remarkable performance, achieving a
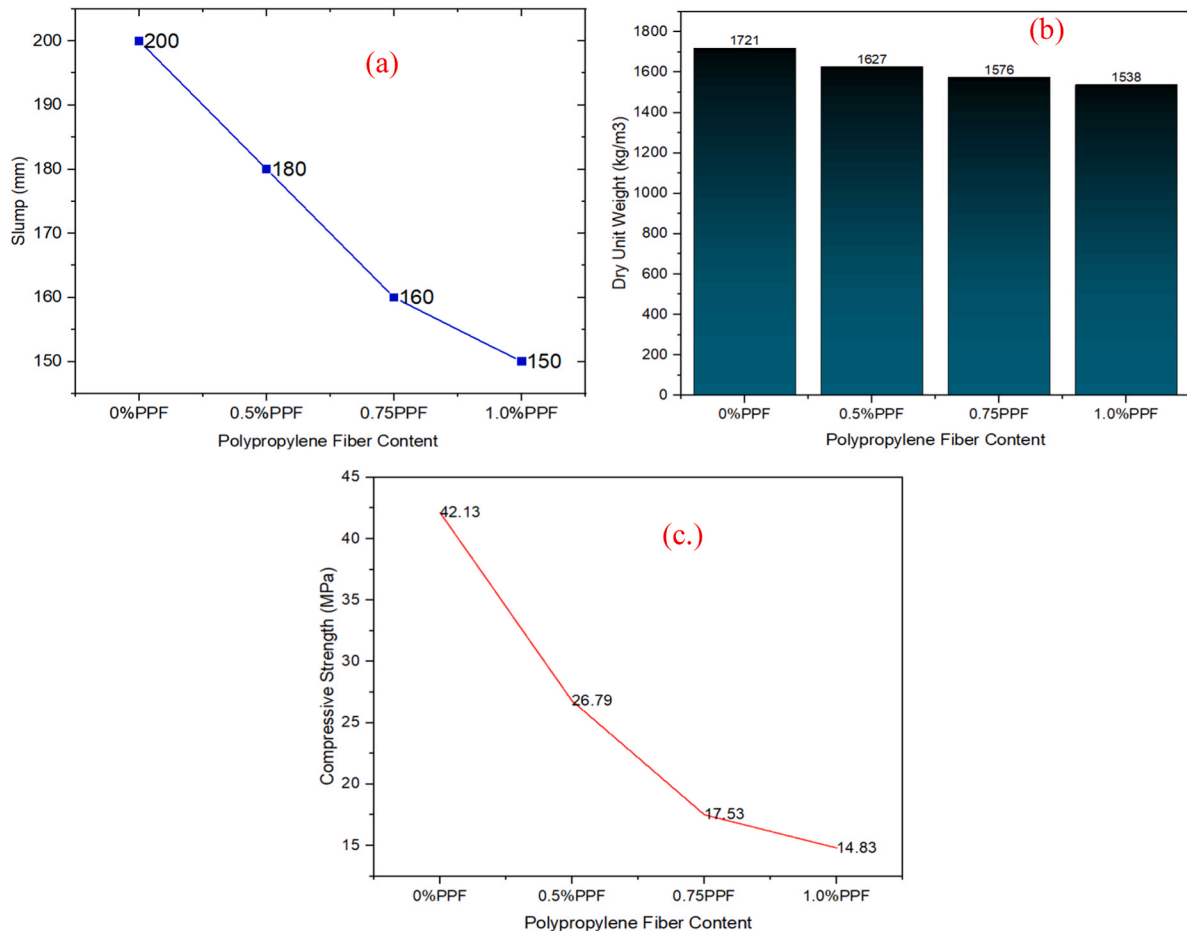

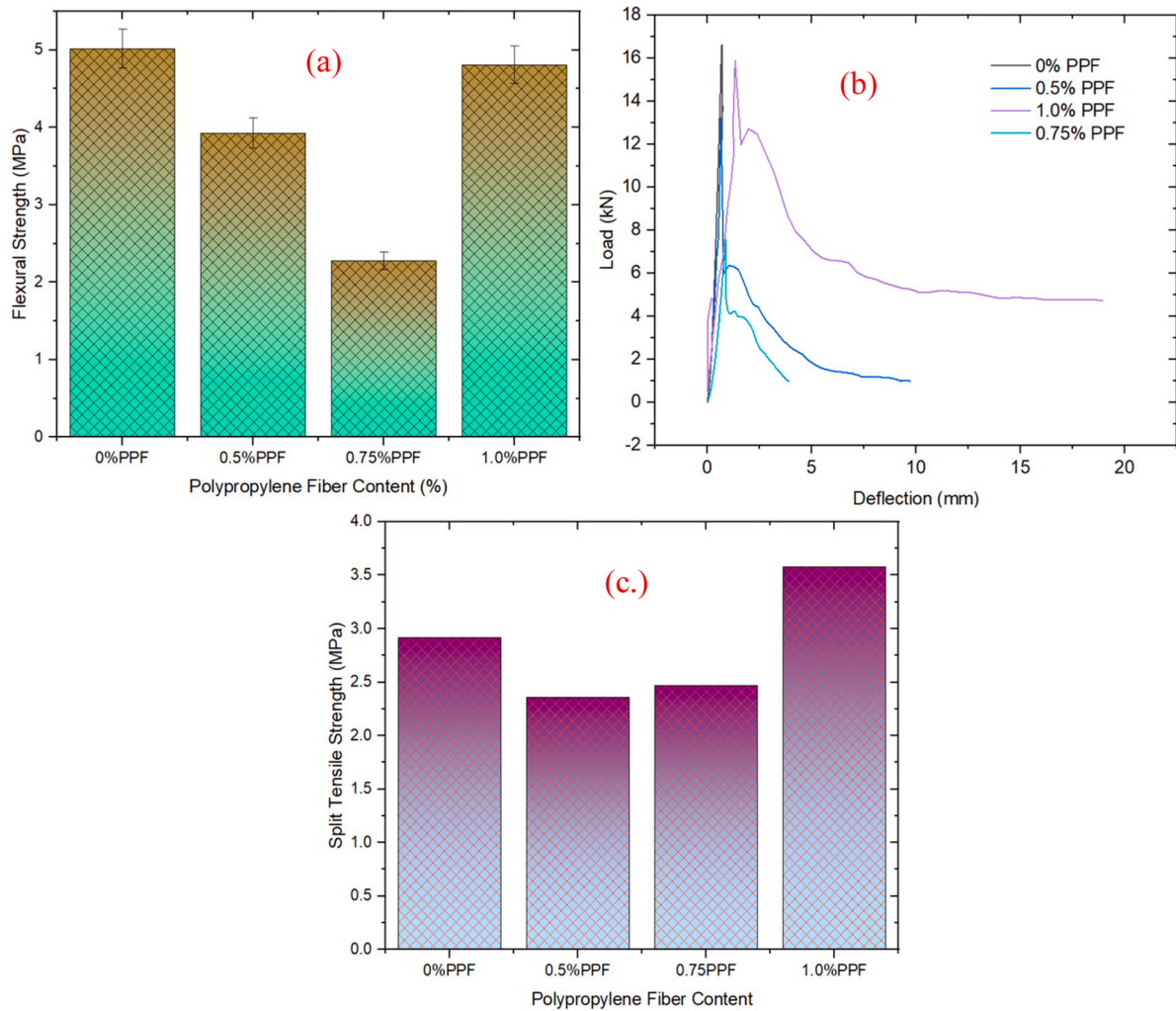Fig. 4. Slump, dry density and compressive strength of LECA fibre-reinforced concrete.

Fig. 5. Flexure and Split tensile strength of fibre-reinforced LECA concrete.
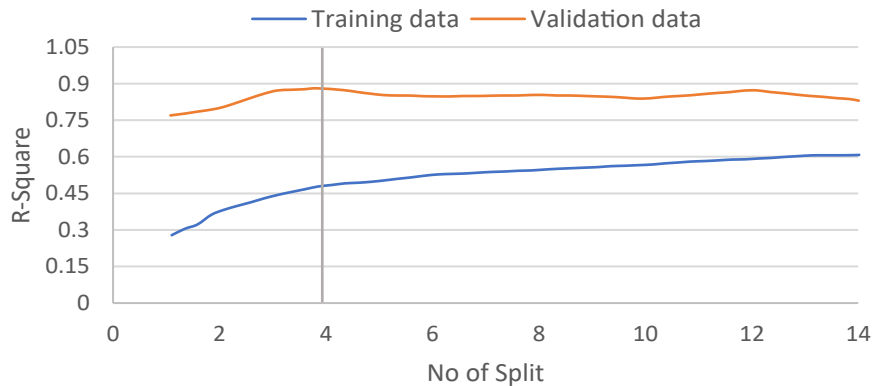

Fig. 6. Splitting history of data for the ANN model.

also enhancing the particle parking through the formation of excess calcium silicate hydrate (C-S-H) gel. This approach addresses the concerns regarding the trade-off between energy absorption capability and other associated structural properties, as noted in previous studies.

1.1. Significance of study

The study employed ANN and RSM techniques to investigate the structural impact resilience of lightweight fibre-reinforced concrete. It focused on the impact energy absorption, crack resistance relative to compressive strength, and residual strength, considering varying PPF volume fractions and Slab thicknesses. Furthermore, the research explored the correlation between responses under both service and ultimate loading conditions. Considering the improvements observed, these findings will inform the application of lightweight LECA concrete reinforced with PPF in construction, especially related to infrastructural projects, commercial and industrial floors, heavy-duty pavements, protective barriers and blast-resistant structures.

Table 3
Statistical validation of the ANN model.

Measures	Eas	Eau	Crs	Cru
Training				
RSquare	0.9997	0.9998	0.9997	0.9987
RASE	1.9601	2.6808	4.131872	4.6306
Mean Abs Dev	6.9122	2.1341	2.225494	1.1679
LogLikelihood	2.4579	5.0537	2.0279	1.8946
SSE	6.2475	7.024	5.711	5.0638
Validation				
RSquare	0.9999	0.9999	0.9996	0.9974
RASE	4.1555	4.8048	2.4346	1.5479
Mean Abs Dev	3.7975	8.6876	3.1449	1.2461
LogLikelihood	19.9037	26.5923	8.8714	5.7556
SSE	12.8829	17.2155	6.6130	3.6143
Test				
RSquare	0.9990	0.9991	0.9991	0.9981
RASE	14.4275	7.6183	6.22982	2.8081
Mean Abs Dev	11.0591	8.5285	4.9036	3.0604
LogLikelihood	8.6165	6.9751	1.1316	3.4430
SSE	7.0796	2.5791	9.0761	4.1835

Table 4
ANOVA results.

Parameter	E_{as} (Joules)	E_{au} (Joules)	C_{rs} (MPa)	C_{ru} (MPa)
Model Type	Quadratic	Quadratic	Quadratic	Quadratic
R^2	0.9997	0.9998	0.9999	0.9999
Adjusted R^2	0.9995	0.9998	0.9999	0.9999
Predicted R2	0.9980	0.9990	0.9996	0.9998
F-value	332.98	400.15	297.08	93.09
P-value	< 0.0001	< 0.0001	< 0.0001	< 0.0001
A	< 0.0001	< 0.0001	< 0.0001	< 0.0001
B	< 0.0001	< 0.0001	< 0.0001	< 0.0001
AB	< 0.0001	< 0.0001	< 0.0001	< 0.0001
A^2	< 0.0001	< 0.0001	< 0.0001	< 0.0001
B^2	< 0.0001	< 0.0001	< 0.0001	< 0.0001

2. Materials used and procedures

2.1. Materials

Grade 42.5 Ordinary Portland Cement (OPC) following Malaysian Standard MS 522 [43] was used to manufacture both plain and fibre-reinforced lightweight concrete. The oxide composition of the cement and micro silica determined using X-ray Fluorescence is presented in Table 1.

Other materials used include LECA, fibrillated PPF and micro-silica. The LECA sizes as shown in Fig. 1(a) range between 4 – 20 mm as provided in ASTM C33/C33 M, with a density of 720 kg/m³. Fig. 1(b) 4.75 mm demonstrates the well-graded fine aggregate distribution.

The polypropylene fibre (PPF) used is the fibrillated type 19 mm in length and has a diameter of 0.75 mm, resulting in an aspect ratio of 25.33. Furthermore, it has a specific gravity is 0.9 kg/m³, with a tensile strength and Young's modulus of 400 MPa and 1150 MPa, respectively. Sika Viscocrete-2192, a polycarboxylic ether, is used as the superplasticizer [44]

2.2. Design of experiment and concrete mix design

2.2.1. Design of experiment

The two main variable constituents in the study polypropylene fibre (PPF) and Slab thicknesses were used to design the experiment utilising the optimal design method available in Version 13: 2021 of the Design Expert software. The choice of the design expert software is due to its flexibility. The PPF is defined as a continuous variable with contents ranging from 0 % to 3 %, while slab thickness is defined as a four-level discrete, consisting of 30 mm,40 mm, 50 mm and 60 mm to allow for an

accurate representation of the responses.

The study considered Polypropylene Fiber (PPF) and Slab Thickness as factors, while crack resistance ratio, Impact energy absorptions, and crack resistance at service and ultimate state are analysed as the responses. The detailed factors from the experimental design are presented in Table 2. Regression models were also developed and validated using ANOVA in the same software.

2.2.2. Concrete mix design

A grade 30 MPa structural lightweight concrete was used in this study, designed according to established LECA mix design guidelines [45]. The plain concrete constituents include 506.19 kg of cement, 546.69 kg of fine aggregate, and 582.12 kg of coarse aggregate (LECA), with a 0.36 water-cement ratio. Additionally, 2.5 % superplasticiser, 10 % micro-silica, and a varying volume fraction of polypropylene fibre content ranging from 1 % to 3 % were used. Based on the experimental design (detailed in Section 2.2.1), 108 slab specimens of thicknesses ranging from 30 mm to 60 mm were produced, 3 specimens for each of the 36 fibre components, shown in Table 2. The results of each run (mix) were analysed for their correlational influence on concrete properties.

2.2.3. Concrete preparation

Since the LECA replaced natural aggregate in the concrete, the overall density was maintained between 1500 kg/m3 and 1800 kg/m³. To improve the ITZ of the final concrete, the LECA was fully saturated with portable tap water for 24 h and dried for 2 h to ensure saturated dry surface condition before being used in the mix. Soaking the LECA minimizes loss of workability and enhances bonding with the cement paste, which in turn improves the concrete's strength. Furthermore, it was anticipated that the synthesis of more C-S-H from micro-silica would fill the ITZ micro-pore.

The cement, sand, and LECA were properly mixed before sprinkling the fibre to ensure adequate distribution, followed by water, micro silica and superplasticizer. Once a homogeneous mix is achieved concrete is placed in a lubricated formwork (300 mm x 300 mm) and allowed to cure under room temperature. Subsequently, formwork is removed and specimens submerged in a water bath for 28 days.

2.3. Experiments

2.3.1. Densities and compressive strengths of fibre reinforced LECA concrete

The density of the LECA concrete was assessed in accordance with the guidelines set forth by ASTM C642. To facilitate this assessment, a representative sample of the hardened LECA concrete was oven-dried at 110 °C until a constant weight (W_d) was achieved. Subsequently, the oven-dried specimen was submerged in clean water at room temperature for 24 hours, and weighed after being surface-dried with a damp cloth (W_{ssd}). The specimen was then re-weighed while suspended in water (W_s). The concrete's dry density was computed using Eq. (1).

$$Dry\ Density = \frac{W_d - W_{ssd}}{W_S} \qquad (1)$$

The compressive strength of the LECA concrete with 0 %, 0.5 %, 0.75 % and 1.0 % volume fractions of PPF was assessed by crushing 150 mm square concrete cubes using a universal testing machine, following ASTM C39 [46]. A gradual compressive loading rate ranging between 0.01 – 0.03 MPa/sec was applied to each specimen. For each PPF content, three specimens were prepared and tested to determine the average compressive strength.

2.3.2. Split tensile and flexural strength

The split tensile strength offers valuable insight into the shear resistance capability of concrete. This strength was assessed by applying a diametral compressive load along the length of a 150 mm cylindrical concrete specimen, following the guidance outlined in ASTM C496 [47].
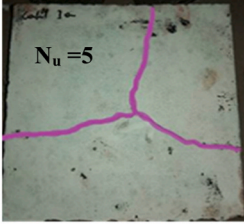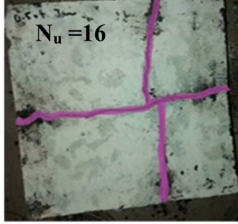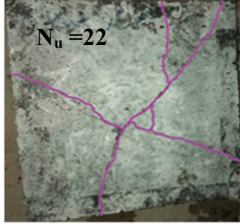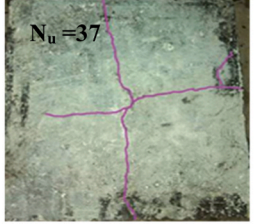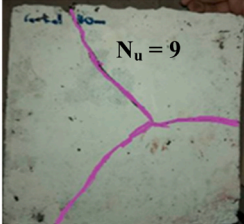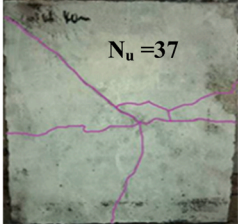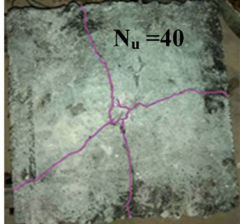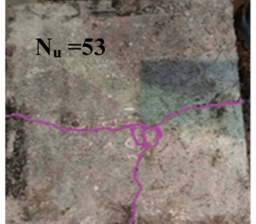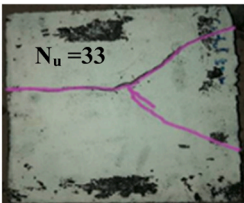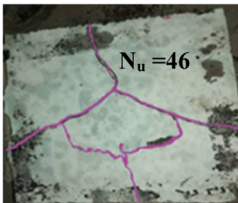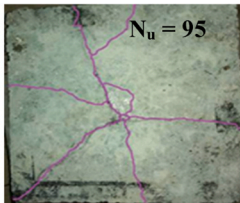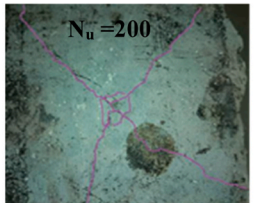
Slab	Volume fraction of PPF (%)			
(mm)	0	0.5	0.75	1.0
30	$N_u = 5$	$N_u = 16$	$N_u = 22$	$N_u = 37$
40	$N_u = 9$	$N_u = 37$	$N_u = 40$	$N_u = 53$
50	$N_u = 33$	$N_u = 46$	$N_u = 95$	$N_u = 200$

Fig. 7. Specimens crack pattern of LECA PPF-reinforced concrete Impact Energy Absorption.

The loading rate was consistently maintained within the range of 0.0012 – 0.0233 MPa/sec.

Furthermore, the flexural strength of the concrete was determined through a 3-point bending test conducted on a 500 mm x 150 mm x 150 mm concrete beam, as specified in ASTM C78 [48]. During the test, the loading rate was maintained between 0.015 – 0.02 MPa/sec.

2.3.3. Impact resistance test

The low-velocity impact test based on ACI 544–2 R[49], was used to investigate the combined varying effects of PPF and slab thickness on the impact energy absorption, crack resistance, and overall damage mechanism of the proposed LECA concrete. 300 mm square concrete slab specimens in 30 mm, 40 mm, 50, and 60 mm thicknesses are utilized. To replicate a low-velocity impact scenario on the specimen's frontal surface, a cylindrical steel ball is dropped from a regulated height for each specimen, as shown in Fig. 2. The specimens are adequately placed on the test frame, thus providing support on four sides.

The weight of the cylindrical balls and the heights of fall were adjusted according to the fibre content and slab thickness in order to correspondingly access the lightweight concrete's impact resistance and crack resistance capabilities. Samples without PPF were subjected to impact from cylindrical steel ball weighing 0.509 kg and falling through a height of 0.5 m, while cylindrical balls weighing 1.05 kg with varying heights of fall of 0.48 m, 0.58 m, and 0.68 m were used for specimens containing fibre contents of 0.5 %, 0.75 %, and 1.0 %, respectively. This enables a scenario with different slab thicknesses and PPF contents that are proportionate in terms of impact and potential energy. Eqs. (2) - (8) were used to calculate the responses at service and ultimate loading based on the number of blows and the cylindrical ball drop height that caused service and ultimate cracks in each example [16,28,49]

$$e = mgh \tag{2}$$

Where m is the ball mass, g is 9.81 m/s^2, h is the height at which the ball is dropped, and e is the energy of blow (Joules).

$$E_{as} = N_s * e \tag{3}$$

$$E_{au} = N_u * e \tag{4}$$

The Ultimate energy absorption is denoted by E_{au}, whereas the service energy absorption is denoted by E_{as} in Eqs. 3 and 4. N_u is the number of blows when the sample failed (i.e., at ultimate cracks), while N_s is the number of blows until the service crack.

$$C_{rs} = E_{as} / \quad (l_c * Cr_{max} * C_w) \tag{5}$$

$$C_{ru} = E_{au} / \quad (l_c * T * C_w) \tag{6}$$

Service and crack resistance are represented by C_{rs} and C_{ru} in Eqs. 5 and 6. T is the specimen thickness, C_w is the maximum crack width, l_c is the total length of all cracks, and Cr_{max} is the maximum crack resistance.

The service and ultimate crack resistance ratio are computed through Eqs. 7 and 8.

$$CR_s = C_{rs} / \quad f_{cu} \tag{7}$$

$$CR_u = C_{ru} / \quad f_{cu} \tag{8}$$

Where CR_s is the Service Impact crack resistance ratio, CR_u is the Service Impact crack resistance ratio, while f_{cu} is cube compressive strength.

Furthermore, to easily evaluate quantitatively the improvement in the impact resistance characteristics; the impact residual strength ratio
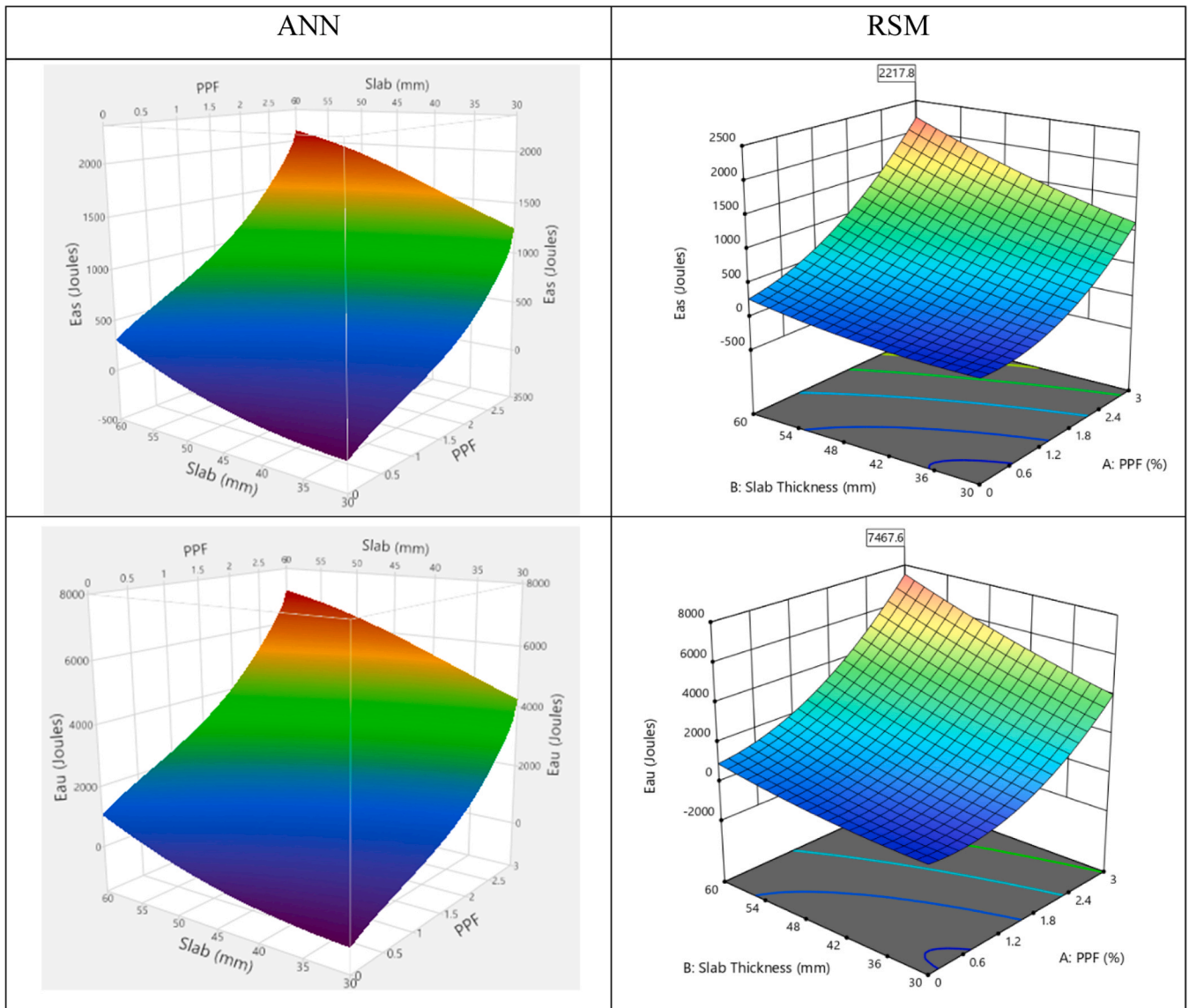
Fig. 8. Impact energy absorptions.

(I_{RS}) was formulated as the ratio of ultimate impact energy to service impact energy as given in Eq. 9 [50].

$$I_{RS} = C_{rs} / \ C_{ru} \tag{9}$$

Where I_{RS} represent the Impact residual strength ratio.

In this context, the I_{RS} serves as a valuable tool for evaluating the post-crack behaviour of the composites and can also be regarded as an indicator of the ductility imparted to the composite by the fibres integrated into the matrix.

3. Model development

3.1. ANN model

The development of the ANN model in this study was implemented using Version 17: 2022 JMP pro software due to its flexibility and robustness. A Multilayer Perceptron (MLP) ANN model of the structure 2–6–6 was developed, consisting of 2 input layers, 6 hidden layers (3 and 3) and 6 output layers as shown in Fig. 3. The MLP was adopted due to its reported excellent performance [51–53]. The PPF and slab thickness are defined as the input parameters while service impact energy absorptions

(E_{as}), ultimate impact energy absorptions (E_{au}), service crack resistances (C_{rs}), ultimate service crack resistances (C_{ru}) are defined as the output, crack resistance ratios at service ($CR._{rs}$) and ultimate loading ($CR._{ru}$) respectively.

To arrive at the optimal 2:6:6 ANN model structure, that is, a model with high learning capacity, the experimentally designed results were partitioned into 60 %, 20 %, and 20 % for training, validation and testing respectively. For each partition, the relationship between training, validation and testing data was accessed in terms of the number of splits and compared with the coefficient of determination (R^2), thereafter the optimum model corresponding to the split with the highest R^2 was adopted.

The K-Fold validation method with 3 seed random reproducibility was utilised, with the TanH activation sigmoid to determine the number of hidden layer structures. A boosting learning rate of 0.1 was adopted with 1 no. of tours as the fitting option.

3.2. Response surface methodology

Response surface methodology (RSM) is a highly effective approach that is widely utilised across various fields today. It comprises a set of mathematical and statistical techniques designed for modelling,
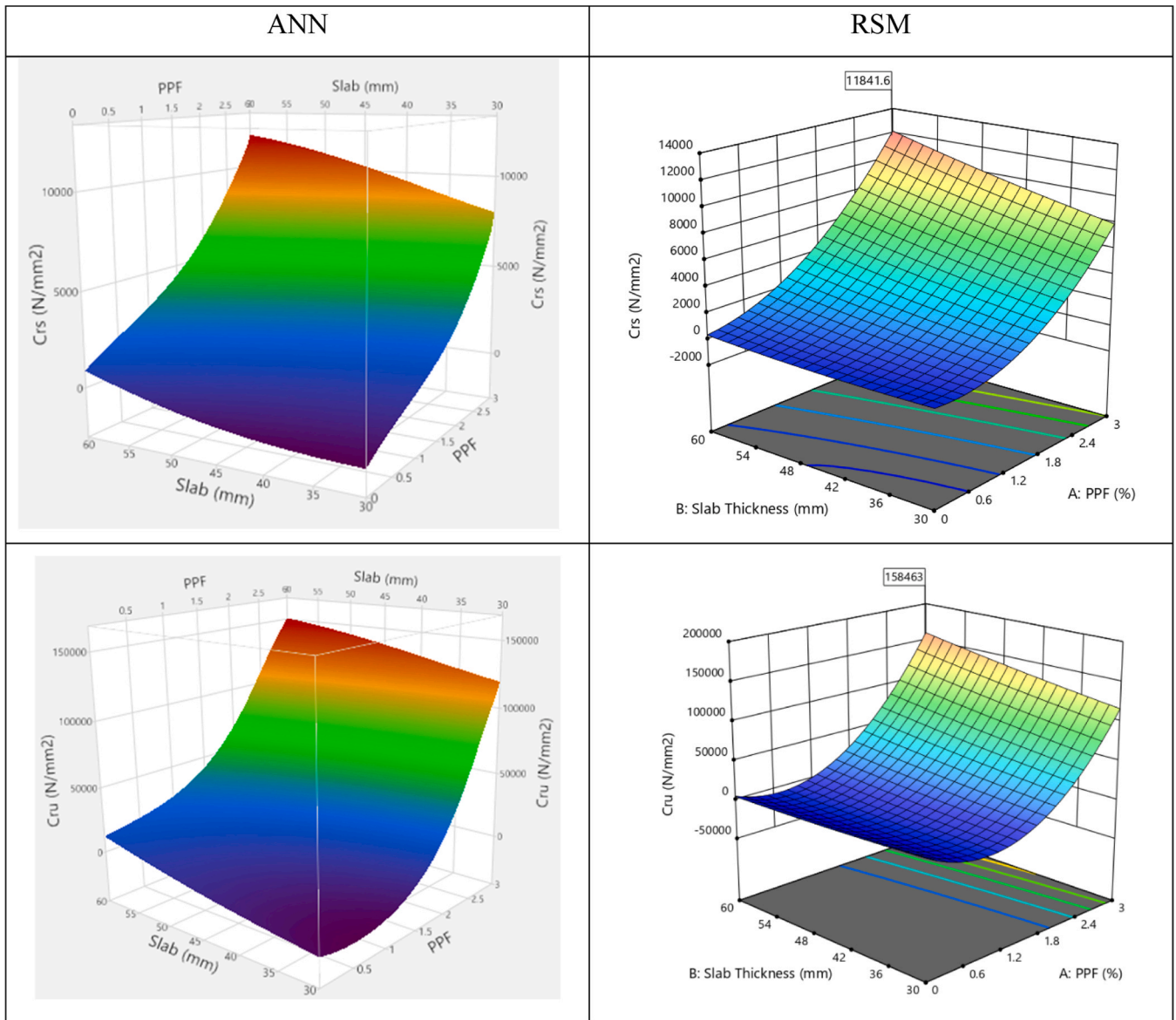
Fig. 9. Crack resistance of lightweight LECA concrete.

evaluating the effects of multiple variables, and optimization [54]. Traditionally, RSM relies on experimental data; however, observational data can also be considered an alternative [55]. The most commonly used software options for RSM include design expert software, Minitab, and XLSTAT. For this study, version 13:2021 of Design-Expert has been selected due to its flexibility. The correlational relationship of factors and responses is represented through contours and surface profilers, effectively illustrating their relationship.

The optimal design method, derived from 2-factorial designs, was utilised for its flexible structure, which allows customization of the models. PPF and Slab thicknesses are the factors under consideration. The results are analysed further using ANOVA and diagnostic assessments. Based on the relationship between the responses and factors, various models- such as quadratic, linear or cubic - are proposed as illustrated in Eqs. (10) and (11).

$$f = A_0 + A_1x_i + A_2x_{ii}... A_nx_n + \varphi \qquad (10)$$

Where f and x represent the factor x and variable respectively. Also, A_0 is the intercept at $x_i = x_j = 0$, A is the coefficients.

$$f = A_0 + \sum_{i=1}^{n} A_i x_i + \sum_{i=1}^{n} A_{ii} x_i^2 + \sum_{i=1}^{n-1} \sum_{j>1}^{n} A_{ij} x_i x_j + \varphi \qquad (11)$$

i is the linear and j is the quadratic quantities, while n represent a numerical variable.

For each analysis, results from ANOVA demonstrate variability between the impact resilience parameters of the concrete specimens, assessed for statistical significance with a 95 % confidence level. Each analysis evaluates the statistical significance of $p - value \leq 0.05$. The lack of fits, variations between adjusted and predicted coefficient of determinations ($R^2_a and R^2_p$) standard deviations are also considered.

3.3. Model performance metrics

The prediction performances of the ANN model were evaluated using four statistical metrics, namely the sum of Square Errors (SSE)coefficient of correlation (R^2), Root Average Squared Error (RASE), and Mean Absolute Deviation (MAD). The R^2 highlights the proportion of the variance in the response variable of the model, the value ranges from 0 to 1, and the closer it is to 1 the better. On the other hand, the RMSE tells us
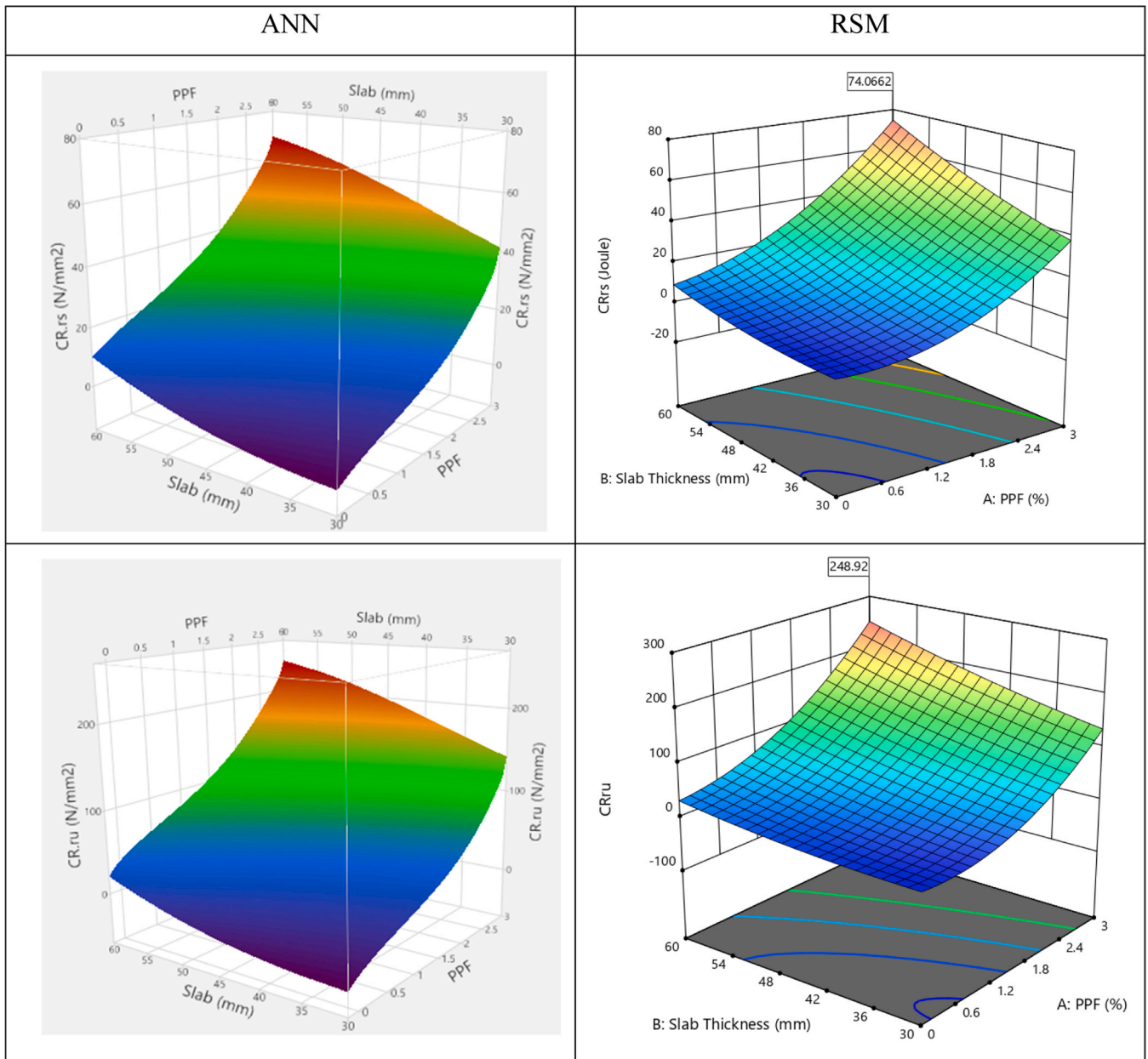
Fig. 10. Surace profile representation of Crack resistance ratio at service and ultimate loading.

how far apart the predicted result is from the original. The MAD measures the variability that indicates the average distance between observations and their mean, while the SSE measures the random error, or the unexplained variation. This is crucial for understanding the output's consistency with the target values. The statistical performance metrics were computed using Eqs. (12) – (15).

$$R^2 = 1 - \frac{\sum_{i=1}^{n}(\text{Re}_i - Rp_i)^2}{\sum_i^n Rp_i^2} \qquad (12)$$

$$MAD = \frac{\sum |x_i - \mu|}{n} \qquad (13)$$

$$RASE = \sqrt{\frac{1}{n}\sum_{i=1}^{n}(\text{Re}_i - Rp_i)^2} \qquad (14)$$

$$SSE = \sum(Y - \widehat{Y})^2 \qquad (15)$$

4. Results and discussion

4.1. Dry unit weight, workability, and compressive strength

Fig. 4 demonstrates a general declining trend in workability (Fig. 4a), which decreases by approximately 10 %, as well as in dry unit weight (Fig. 4b), which declines by about 3.8 % for each 0.25 % increment in PPF volume fraction. Furthermore, compressive strength is noted to decrease by about 65 % (Fig. 4c). While the reduction in dry unit weight is impressive, indicating that the inclusion of more PPF leads to lighter LECA concrete, this benefit comes at the expense of workability. Consequently, a higher w/c ratio becomes necessary, leading to a further reduction in compressive strength.

The decreased workability is a consequence of the increased contact surface area between the cement matrix, LECA and the PPF, leading to higher resistance to flow within the concrete mix, as confirmed by previous study [56]. The decrease in dry unit weight can be attributed to
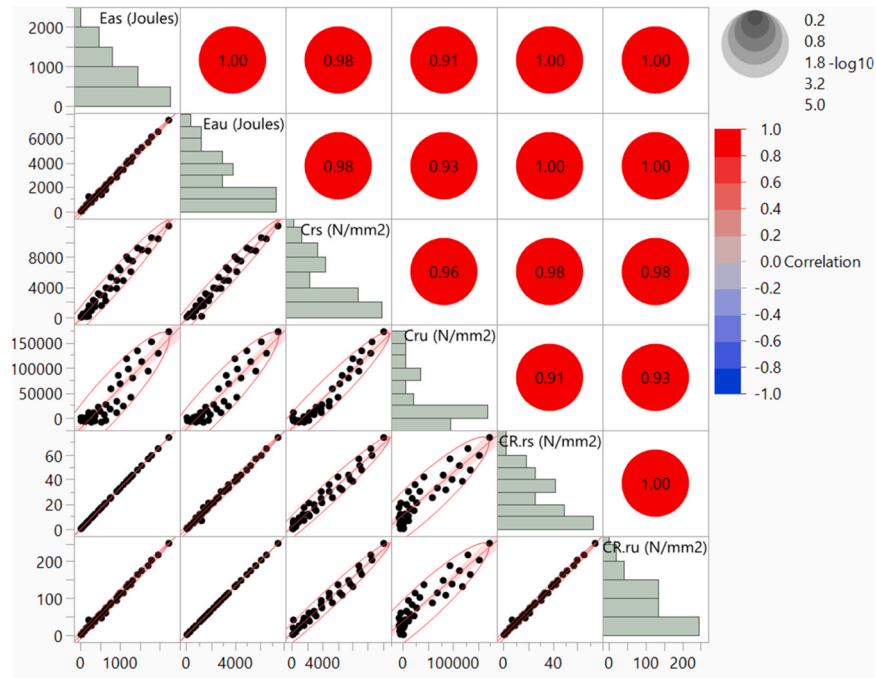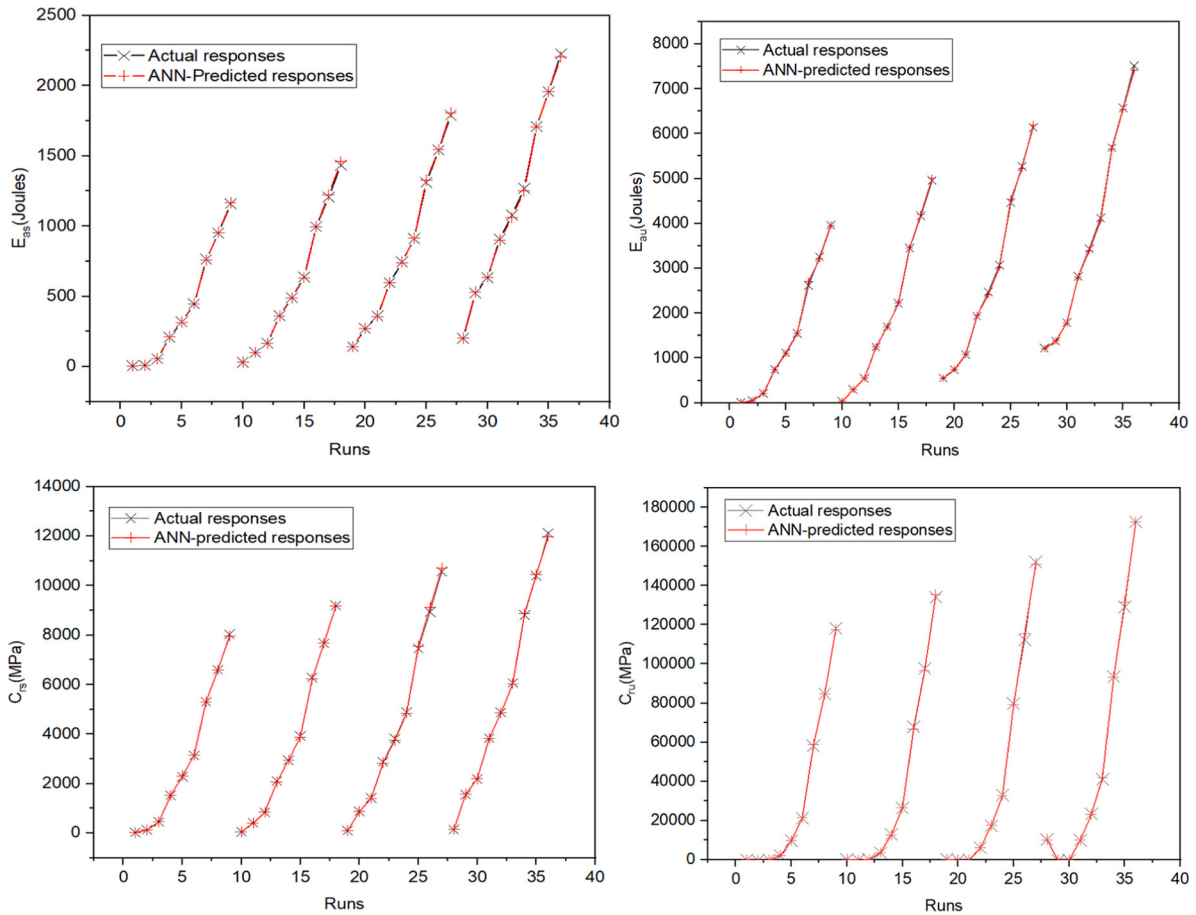
Fig. 11. Correlation of ANN-predicted responses.

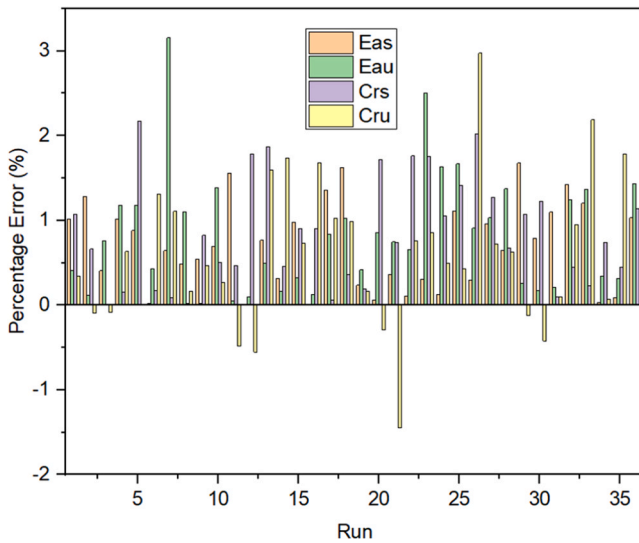**Fig. 12.** Comparison between actual and ANN-predicted responses.

Fig. 13. Percentage error between RSM and ANN-Predicted responses.

the higher void content within the concrete associated with the LECA, as confirmed by another study [57].

On the other hand, the decrease in compressive strength is attributed to LECA's inability to withstand the anticipated 60 %-75 % compressive load [58,59] typically expected from coarse aggregate in concrete. While this observation may be subjective to the type of LECA used in this study, it highlights the limitations of fully substituting natural aggregates with LECA as coarse aggregates due to its inherent porosity. Furthermore, the possibility of a weak bond between LECA, PPF and the cement paste could contribute to this phenomenon, resulting in increased porosity around the ITZ and subsequently affecting load transfer and leading to more rapid crushing of the LECA, ultimately culminating in concrete failure [60]. The influence of PPF on density is demonstrated in Fig. 4(c).

4.2. Flexural and split tensile strength

Fig. 5(a, b and c) depicts the flexural and split tensile behaviour of LECA concrete containing varying PPF volume fractions. It was observed that incorporating PPF content of up to 0.75 % negatively affected both responses. Nonetheless, a notable enhancement of 90 % was noted when PPF content increased from 0.75 % to 1.0 %, indicating that a higher

level of PPF enables the concrete to better withstand increased flexural loadings. Furthermore, the load-displacement curve (Fig. 5b) reveals that all samples containing PPF exhibit improved performance beyond their ultimate strength, effectively delaying crack manifestation.

In contrast, the control specimen without PPF (0 %PPF) demonstrates a sudden drop in the curve, indicating immediate failure after attaining its ultimate strength. Consequently, the sample containing 1 % polypropylene fibre demonstrated superior load-deflection performance, yielding a 180 % improvement in crack resistance, although accompanied by a corresponding 5 % decrease in ultimate strength. These findings are in agreement with previous studies [60,61].

A trend similar to that observed in flexural strength is also evident in the split tensile strength, as shown in Fig. 6(c). When the PPF content is below 1.0 %, there is a significant decline in performance. However, when increased to 1.0 % PPF, there is an increase of approximately 23 %. This infers that 1.0 % PPF optimally bridges the cracks and distributes stress more evenly throughout the concrete [16,60,62].

4.3. Model performance

4.3.1. ANN

The data is portioned into training, validation and testing using the decision tree technique. The split history shown in Fig. 6 demonstrates no further improvements in the validation dataset after four splits. The value of R^2 of 0.8812 obtained with these four splits supports the model as a robust predictor of the response. Overall, the R-square values for the model are in the range of 0.99 as shown in Table 3.

4.3.2. RSM

The statistical result shown in Table 4 demonstrates reasonable agreement, with all p-values maintained below the allowable threshold of 0.05. Additionally, the variation between predicted R^2 and adjusted R^2 is significantly low, < 0.2, a measuring criterion according to the design expert manual - Version 13:2021. The experimental results are also analysed using the same software using response surface methodology.

4.4. Analysis of responses

4.4.1. Specimen failure pattern under impact loading

Fig. 7 presents the crack patterns observed in LECA concrete slab specimens of varying PPF content and thicknesses when subjected to proportional low-velocity impact loading. A detailed examination indicates that, although the crack patterns are largely consistent, there is a
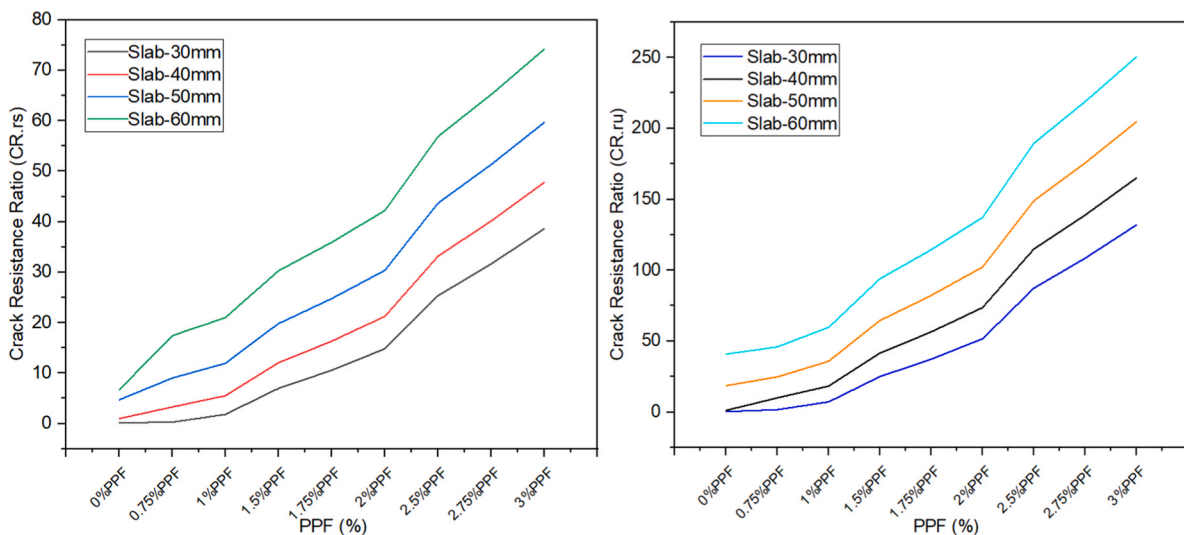

Fig. 14. Variation of crack resistance relative to compressive strength.
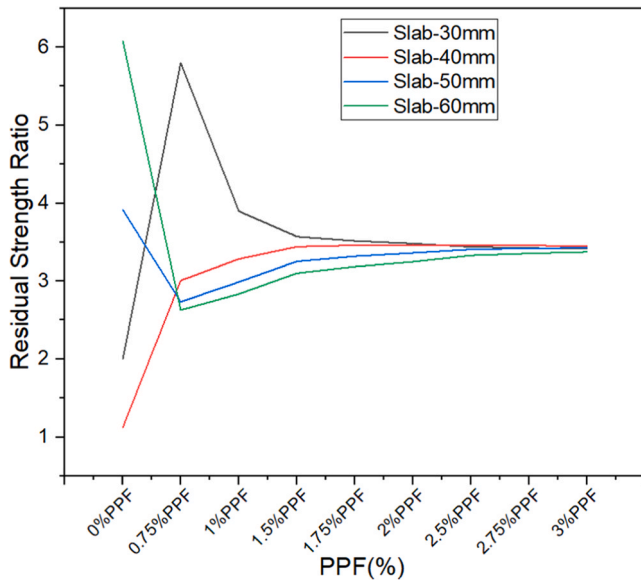
Fig. 15. Residual strengths.

notable increase in the number of blows sustained before ultimate failure with each increment in the slab thickness and PPF volume fraction. This enhancement in the number of accommodated blows accommodated reflects an improvement in the overall structural impact resilience, specifically the energy absorption capacity of the concrete, thereby increasing its crack resistance. These findings are in line with those reported in previous studies [62–64].

4.4.2. Impact energy absorptions

The figures depicted in Fig. 8 demonstrate the energy absorption capabilities of the lightweight fibre-reinforced LECA slab concrete under ultimate impact loadings. These plots highlight the significant influence of varying PPF and slab thickness on the concrete's impact resilience performance. Eqs. 16 and 17 are the predictive models for the observed responses. The results indicate a consistent enhancement with increasing PPF content at both service and ultimate loading, reiterating the ability of the LECA aggregate to withstand impact loading. Specifically, the optimal energy absorption values of 2205.9 Joules and 7404.9 Joules were attained with the 60 mm thick slab containing 3 % PPF, representing an impressive improvement of 11 times and 33 times, respectively. The responses generated by both ANN and RSM are aligned, further validating the accuracy of both models.

$$E_{as} = 387.95 - 362 * PPF - 24.05 * ST + 9.06 * PPF * ST + 157.31$$
$$* PPF^2 + 0.37 * ST^2 \tag{16}$$

$$E_{au} = 1027.25 - 1347.15 * PPF - 63.23 * ST + 28.26 * PPF$$
$$* ST + 610.35 * PPF^2 + 1.04 * ST^2 \tag{17}$$

The influence of PPF becomes increasingly pronounced as the slab thickness increases, as evidenced by a gradual transition in colour from blue to cyan, green, yellow-orange, and finally red. A significant enhancement is noted when PPF exceeds 2 %, suggesting an improved capacity for impact absorption in the specimens. Conversely, PPF% below 0.6 % show no contribution to this improvement.

The length of fibres, the efficient fusion of LECA, and the subsequent densification of the microstructure due to the increased C-H-S produced from micro-silica are some of the key factors responsible for the observed improvements. Another study demonstrated relevant improvements in the impact resistance of 2-way slabs containing 0.9 % PPF content [65]. Comparable gains have also been reported in other studies

involving steel and basalt fibre [62,64,66]. Furthermore, it has been noted that incorporating up to 10 % silica fume into concrete significantly boosts the compressive, tensile, and flexural strengths of LECA concrete [67].

4.4.3. Crack resistance

The 2D contour plots presented in Fig. 9 illustrate the influence of slab thickness and PPF content on crack resistance under different stages of impact loading. Eqs. 18 and 19 are the developed prediction models for these responses. An increase in both PPF and slab thickness leads to enhanced crack resistance, achieving optimal values of 11930 MPa at service and 170337 MPa at ultimate loading conditions. This signifies an 83-fold and 17-fold enhancement in the service and ultimate performance of the control sample without PPF. However, it is worth noting that PPF contents of up to 0.6 % and 1.5 % negatively impact the service and ultimate crack resistance of the concrete, respectively.

$$C_{rs} = 1214.12 - 1876.23 * PPF - 65.83 * ST + 42.57 * PPF$$
$$* ST + 1084.86 * PPF^2 + 0.86 * ST^2 \tag{18}$$

$$C_{ru} = 38142.47 - 71507.49 * PPF - 1054.55 * ST + 577.59 * PPF$$
$$* ST + 29497.87 * PPF^2 + 8.43 * ST^2 \tag{19}$$

The observed improvement in the crack resistance behaviour is due to the high tensile stress properties of the PPF, which effectively inhibit both the initiation and propagation of cracks, especially as the thickness of the slab increases [68]. Furthermore, evidence suggests that longer fibres exhibit greater resistance to cracking [69].

4.4.4. Crack resistance ratio

The crack resistance ratio quantifies the effectiveness of the concrete to resist cracking relative to its compressive strength. Fig. 10 demonstrates the predicted relationships of the specimen with varying thicknesses and PPF under service and ultimate loading state. Eqs. 20 and 21 are the predictive models of the responses.

$$CR_{rs} = 12.93 - 12.07 * PPF - 0.80 * ST + 0.30 * PPF * ST + 5.25$$
$$* PPF^2 + 0.01 * ST^2 \tag{20}$$

$$CR_{ru} = 34.24 - 44.91 * PPF - 2.11 * ST + 0.94 * PPF * ST + 20.35$$
$$* PPF^2 + 0.03 * ST^2 \tag{21}$$

In both ANN and RSM surface profiles, thicknesses below 36 mm containing less than 0.6 % PPF demonstrate no crack resistance completely relative to the compressive strength when subjected to service loading. However, an improvement is observed with increases in both PPF and thicknesses, with the PPF having a slightly greater influence. On the other hand, at ultimate loading, the concrete shows enhancement throughout compared to the control sample.

4.5. Multivariate analysis of ANN predicted responses

Fig. 11 demonstrates the correlation matrix of the predicted responses. The upper triangle plot is completely red, indicating a high correlation between energy absorptions and crack resistance, and crack resistance ratios of the concrete at both service and ultimate states. The perfect fit in the lower triangle plot further supports this. The least correlation of 0.91 can be seen to exist between service impact energy absorptions and ultimate crack resistance. In general, the plot indicates that the increase in each of the responses increases other responses.

4.6. Comparison of ANN-predicted and RSM responses

A direct comparison between all actual and predicted responses on all thirty-six runs as shown in Fig. 12 reveals a strong agreement with predicted mean deviations of 0.2 %, - 0.22 %, 0.18 % and 0.12 % for

service impact energy absorption, ultimate energy absorptions, service crack resistance, and ultimate crack resistance respectively.

Moreover, the plot trend reveals the correlational significance of the two factors; PPF and slab thickness on the Eas, Eau, Crs, and Cru. The PPF is seen to influence the increase of all the responses significantly. These results further demonstrate the robustness of the proposed ANN model.

Fig. 13 shows the percentage of error between the RSM and ANN-predicted responses. The highest increased variation is about 3.1 % at Run 8 with the highest decrease of about −1.5 % at Run 23. These variations are attributed to the limited number of data considered. Nonetheless, the general prediction performance of about 95 % is achieved with less than 2 % variation. These affirm the robustness of the ANN as a strong prediction tool as confirmed by previous studies [36,38, 40,41].

4.7. Crack resistance ratio relative to compressive strength

Fig. 14 illustrates the variation of the crack resistance ratio of LECA concrete with varying PPF content and slab thickness under service and ultimate impact loading. This relationship demonstrated how effectively the concrete resists cracking relative to the respective compressive strength. The plot shows the increase in crack resistance directly proportional to both PPF and slab thickness at both service and ultimate. Aside from the contribution of the PPF in enhancing the toughness of the concrete, the LECA as a coarse aggregate has successfully withstood the anticipated 60 % - 75 % compressive loading.

4.8. Residual strength ratio

The residual strength ratio (Irs) shown in Fig. 15 is a toughness parameter, computed here as the ratio of ultimate to service impact energy absorptions of the respective specimens to demonstrate the remaining service life of each specimen considering variations in thickness and PPF volume fraction. A closer observation reveals a notable jump in the residual strength of 30 mm and 40 mm specimens with PPF up to 0.75 %, followed by a sharp drop. This behaviour stands in contrast to the results observed in the 50 m and 60 mm slabs. Nonetheless, there remains a consistent residual strength across all specimens with PPF contents ranging between 1.5 % and 3 %.

This consistent performance indicates a reliable level of toughness and energy absorption after cracking, thereby demonstrating the effectiveness of higher fibre content in bridging cracks. These characteristics not only enhance design flexibility for optimising material usage and cost but also ensure that structural integrity remains uncompromised. Furthermore, incorporating PPF in this range can facilitate effective uniform load distribution, thereby reducing the likelihood of localised failures.

It is also observed that the residual strength decreases as the slab thickness increases. Suggesting that the load transfer mechanism, stress distribution and the fibre aspect ratio have a more pronounced effect in thinner slabs, thereby enhancing the overall performance.

4.9. Practical implications and applications

The findings reveal a strong correlation between the structural impact resilience parameters of the LECA concrete considered, demonstrating notable improvements in crack resistance and impact energy absorption in relation to the compressive strength. This is reflected in the residual strength, which, along with the durability, increases in direct proportion to both PPF and slab thickness. Furthermore, this underscores the LECA concrete's ability to withstand harsh conditions and mechanical stresses over time, thereby reducing maintenance costs and extending the life span of the structure. The consistent residual strength observed, ranging from 1.5 % and 3 % across all concrete specimens, shows that even after initial cracking, the concrete can

continue to withstand loads, thereby enhancing the safety of the structures. This aspect is particularly important for structures that need to withstand lateral forces.

In terms of applications, the proposed concrete characterised by its consistent residual strength, is particularly well-suited for infrastructural projects where high durability and impact resistance are crucial, such as highways and tunnels. Furthermore, the concrete's enhanced impact and crack resistance also makes it suitable for commercial and industrial floors, including heavy-duty pavements and parking areas. Furthermore, this concrete can be utilised in precast concrete products, residential construction, and other seismic-resistant structures.

5. Conclusions

The structural impact resilience of lightweight fibre-reinforced LECA concrete has been explored by investigating the crack resistance, impact energy absorptions, and residual strength across different specimens with varying polypropylene fibre contents (ranging from 0 % to 3 %) and slab thicknesses. LECA is used as a complete replacement for natural aggregate in the concrete, effectively reducing the concrete weight. The study focused on square slabs measuring 300 mm, with thicknesses of 30 mm, 40 mm, 50 mm, and 60 mm, subjected to impact loading. The results from 36 experimentally designed mixes, comprising a total of 108 specimens, were analysed using ANN and RSM techniques.

The following conclusions were derived from the findings:

- The inclusion of up to 1 % polypropylene fibre (PPF) resulted in a 3.8 % decrease in concrete density, along with corresponding decreases in both workability and compressive strength of the LECA concrete by 10 % and 65 % respectively.
- Additionally, Increased PPF content and slab thickness led to enhanced structural impact resilience, as evidenced by impact energy absorptions increasing by as much as 33 times and crack resistance by up to 17 times in the lightweight LECA concrete. Indicating the concrete's ability to effectively accommodate minor cracks due to its enhanced load-carrying capacity.
- A strong correlation between crack resistance, impact energy absorptions and crack resistance ratio has been established, demonstrated by high R^2 values of 0.999.
- Crack resistance in relation to compressive strength is directly proportional to both PPF and concrete thickness.
- Consistent residual strength was observed in concrete with PPF content ranged 1.5–3 %
- Interestingly, concrete with lower thickness showed greater residual strength, suggesting effective load transfer and stress distribution influenced by the fibre aspect ratio.

CRediT authorship contribution statement

Ja'e Idris Ahmed: Writing – review & editing, Writing – original draft, Validation, Software, Methodology, Investigation, Formal analysis, Data curation. **Muda Zakaria Che:** Writing – review & editing, Validation, Supervision, Project administration, Methodology, Investigation, Data curation, Conceptualization. **Almujibah Hamad:** Writing – review & editing, Visualization, Validation, Resources, Funding acquisition, Formal analysis, Data curation. **Bashir Maaz Osman:** Visualization, Funding acquisition, Data curation. **Amaechi Chiemela:** Writing – review & editing, Investigation, Formal analysis, Data curation. **Syamsir Agusril:** Visualization, Supervision, Project administration, Investigation, Data curation. **Alengaram U Johnson:** Visualization, Validation, Data curation. **Elshekh Ali A:** Visualization, Resources, Funding acquisition, Data curation.

Declaration of Competing Interest

The authors declare the following financial interests/personal relationships which may be considered as potential competing interests: Hamad Almujibah reports article publishing charges was provided by Taif University. If there are other authors, they declare that they have no known competing financial interests or personal relationships that could have appeared to influence the work reported in this paper.

Acknowledgement

Data availability

The authors do not have permission to share data.

References

[1] K.-C. Thienel, T. Haller, N. Beuntner, Lightweight concrete—from basics to innovations, Materials 13 (5) (2020) 1120 [Online]. Available: https://www.mdpi.com/1996-1944/13/5/1120.
[2] B. Vinod, H. Surendra, R. Shobha, Lightweight concrete blocks produced using expanded polystyrene and foaming agent, Mater. Today.: Proc. 52 (2022) 1666–1670.
[3] M. Kadela, A. Kukiełka, M. Małek, Characteristics of lightweight concrete based on a synthetic polymer foaming agent, Materials 13 (21) (2020) 4979.
[4] A.H. Abdullah, S.D. Mohammed, The fire effect on the performance of reinforced concrete beams with partial replacement of coarse aggregates by expanded clay aggregates, Eng., Technol. Appl. Sci. Res. 13 (6) (2023) 12220–12225.
[5] N.F. Zamri, R.N. Mohamed, D. Awalluddin, S. Mansor, (Year).Palm oil clinker as coarse and fine aggregates in lightweight concrete. AWAM International Conference on Civil Engineering, Springer, 2022, pp. 223–233.
[6] M. Maghfouri, et al., Drying shrinkage properties of expanded polystyrene (EPS) lightweight aggregate concrete: a review, Case Stud. Constr. Mater. 16 (2022) e00919.
[7] S.K. Adhikary, et al., Lightweight self-compacting concrete: a review, Resour., Conserv. Recycl. Adv. 15 (2022) 200107.
[8] P. Pongsopha, P. Sukontasukkul, H. Zhang, S. Limkatanyu, Thermal and acoustic properties of sustainable structural lightweight aggregate rubberized concrete, Results Eng. 13 (2022) 100333.
[9] Y.M. Hussein, M. Abd Elrahman, Y. Elsakhawy, B.A. Tayeh, A.M. Tahwia, Development and performance of sustainable structural lightweight concrete containing waste clay bricks, J. Mater. Res. Technol. 21 (2022) 4344–4359.
[10] M.M. Atyia, M.G. Mahdy, M. Abd Elrahman, Production and properties of lightweight concrete incorporating recycled waste crushed clay bricks, Constr. Build. Mater. 304 (2021) 124655.
[11] S. Rattanachan, C. Lorprayoon, Korat clays as raw materials for lightweight aggregates, Sci. Asia 31 (42) (2005) 277–281.
[12] O. Sengul, S. Azizi, F. Karaosmanoglu, M.A. Tasdemir, Effect of expanded perlite on the mechanical properties and thermal conductivity of lightweight concrete, Energy Build. 43 (2-3) (2011) 671–676.
[13] C.V. Amaechi, et al., Numerical study on plastic strain distributions and mechanical behaviour of a tube under bending, Inventions 7 (1) (2022) 9.
[14] A. Concrete, Guide Struct. Lightweight (1987).
[15] Standard Specification for Lightweight Aggregates for Concrete Masonry Units, C331/C331M, A., West Conshohocken, PA, 19428–2959 USA, 2023. [Online]. Available: https://www.astm.org/c0331_c0331m-17.html..
[16] I.A. Ja'e, et al., Modelling and optimisation of the structural performance of lightweight polypropylene fibre-reinforced LECA concrete, Results Eng. 24 (2024) 103149, https://doi.org/10.1016/j.rineng.2024.103149.
[17] N. Bheel, et al., Enhancing performance and sustainability of GGBFS-based self-compacting geopolymer concrete blended with coal bottom ash and metakaolin by using RSM modelling, Sci. Rep. 14 (1) (2024) 19754, https://doi.org/10.1038/s41598-024-70800-0.
[18] M. Elshahawi, A. Hückler, M. Schlaich, Infra lightweight concrete: a decade of investigation (a review), Struct. Concr. 22 (2021) E152–E168.
[19] T.Y. Lo, W.C. Tang, H.Z. Cui, The effects of aggregate properties on lightweight concrete, Build. Environ. 42 (8) (2007) 3025–3029, https://doi.org/10.1016/j.buildenv.2005.06.031.
[20] J. Jeyanthi, S. Revathi, Study of light weight composite concrete incorporated with polypropylene fiber and cenosphere, Mater. Today.: Proc. 62 (2022) 4303–4309.
[21] S. Iqbal, A. Ali, K. Holschemacher, T.A. Bier, Mechanical properties of steel fiber reinforced high strength lightweight self-compacting concrete (SHLSCC), Constr. Build. Mater. 98 (2015) 325–333.
[22] J. Li, J. Niu, C. Wan, X. Liu, Z. Jin, Comparison of flexural property between high performance polypropylene fiber reinforced lightweight aggregate concrete and steel fiber reinforced lightweight aggregate concrete, Constr. Build. Mater. 157 (2017) 729–736.
[23] C.V. Amaechi, A. Reda, I.A. Ja'e, C. Wang, C. An, Guidelines on composite flexible risers: monitoring techniques and design approaches, Energies 15 (14) (2022) 4982.
[24] R. Prakash, R. Thenmozhi, S.N. Raman, C. Subramanian, N. Divyah, Mechanical characterisation of sustainable fibre-reinforced lightweight concrete incorporating waste coconut shell as coarse aggregate and sisal fibre, Int. J. Environ. Sci. Technol. 18 (6) (2021) 1579–1590, https://doi.org/10.1007/s13762-020-02900-z.
[25] S.P. Yap, U.J. Alengaram, M.Z. Jumaat, Enhancement of mechanical properties in polypropylene–and nylon–fibre reinforced oil palm shell concrete, Mater. Des. 49 (2013) 1034–1041.
[26] Y.O. Özkılıç', et al., Lightweight expanded-clay fiber concrete with improved characteristics reinforced with short natural fibers, Case Stud. Constr. Mater. 19 (2023) e02367, https://doi.org/10.1016/j.cscm.2023.e02367.
[27] L.A. Nour, M. Gamal, A. Ghoniem, Glass fiber for improved behavior of light expanded clay aggregate concrete beams: an experimental study, Frat. Ed. Integrità Strutt. 17 (65) (2023) 1–16.
[28] I.A. Ja'e, et al., Structural performance of lightweight fibre-reinforced oil palm shell concrete subjected to impact loadings under varying boundary conditions, Case Stud. Constr. Mater. 22 (2025) e04240, https://doi.org/10.1016/j.cscm.2025.e04240.
[29] V. Ganesh, N. Divyah, R. Rajkumar, Enhancing structural performance: fiber reinforcement in sintered flyash lightweight concrete for impact resistance and toughness, Indian J. Sci. Technol. 17 (15) (2024) 1577–1585.
[30] F. Jiang, W. Deng, Q. Wang, J. Wang, Z. Mao, Performance research and engineering application of fiber-reinforced lightweight aggregate concrete, Materials 17 (22) (2024) 5530.
[31] J. Esmaeili, M. Ghaffarinia, M. Nodehi, O. Gencel, J. Shi, T. Ozbakkaloglu, Mechanical and fractural characteristics of structural lightweight fiber reinforced concrete, Struct. Concr. 24 (2) (2023) 2420–2439.
[32] W.B. Chaabene, M. Flah, M.L. Nehdi, Machine learning prediction of mechanical properties of concrete: critical review, Constr. Build. Mater. 260 (2020) 119889.
[33] P.G. Asteris, A.D. Skentou, A. Bardhan, P. Samui, K. Pilakoutas, Predicting concrete compressive strength using hybrid ensembling of surrogate machine learning models, Cem. Concr. Res. 145 (2021) 106449.
[34] T.T. Nguyen, L.T. Ngoc, H.H. Vu, T.P. Thanh, Machine learning-based model for predicting concrete compressive strength, GEOMATE J. 20 (77) (2021) 197–204.
[35] J. Ning, Y. Feng, H. Ren, X. Xu, Prediction model for the failure behavior of concrete under impact loading base on back propagation neural network, Constr. Build. Mater. 411 (2024) 134297.
[36] Maqsoom, A. et al.,(2021) Using Multivariate Regression and ANN Models to Predict Properties of Concrete Cured under Hot Weather, Sustainability, vol. 13, no. 18, p. 10164. [Online]. Available: https://www.mdpi.com/2071-1050/13/18/10164.
[37] R. Ramachandra, S. Mandal, Prediction of fly ash concrete type using ANN and SVM models, Innov. Infrastruct. Solut. 8 (1) (2022) 47, https://doi.org/10.1007/s41062-022-01014-4.
[38] Lin, C.-J. and Wu, N.-J.,(2021) An ANN Model for Predicting the Compressive Strength of Concrete, Applied Sciences, vol. 11, no. 9, p. 3798. [Online]. Available: https://www.mdpi.com/2076-3417/11/9/3798.
[39] A. Hammoudi, K. Moussaceb, C. Belebchouche, F. Dahmoune, Comparison of artificial neural network (ANN) and response surface methodology (RSM) prediction in compressive strength of recycled concrete aggregates, Constr. Build. Mater. 209 (2019) 425–436, https://doi.org/10.1016/j.conbuildmat.2019.03.119.
[40] T. Gupta, K.A. Patel, S. Siddique, R.K. Sharma, S. Chaudhary, Prediction of mechanical properties of rubberised concrete exposed to elevated temperature using ANN, Measurement 147 (2019) 106870, https://doi.org/10.1016/j.measurement.2019.106870.
[41] M.J. Moradi, M. Khaleghi, J. Salimi, V. Farhangi, A.M. Ramezanianpour, Predicting the compressive strength of concrete containing metakaolin with different properties using ANN, Measurement 183 (2021) 109790, https://doi.org/10.1016/j.measurement.2021.109790.
[42] Y.X. Tang, et al., Artificial neural network-forecasted compression strength of alkaline-activated slag concretes, Sustainability 14 (9) (2022) 5214.
[43] Portland Cement Specification, 1), M.S.M.P., Malaysia, 2003.
[44] Sika-ViscoCrete-2192, Sika, Malaysia, 2018. [Online]. Available: https://mys.sika.com/content/dam/my01/m/sika_viscocrete_-2192.pdf.
[45] Gobain, L.-S., "Lightweight Aggregate Concrete- Production and Concrete Properties." [Online]. Available: https://www.leca.co.uk/sites/leca.co.uk/files/pdf/1.Leca%20Concrete%20PDF%2010.07.24_0.pdf.
[46] Standard Test Method for Compressive Strength of Cylindrical Concrete Specimens, C39/C39M-20, A., 2005, 2000.
[47] Standard Test Method for Splitting Tensile Strength of Cylindrical Concrete Specimens, C496/C496M-17, A., 2017.
[48] Standard Test Method for Flexural Strength of Concrete (Using Simple Beam with Third-Point Loading), C78-09, A., 2010.
[49] R-89, A.,(1999) Measurement of properties of fiber reinforced concrete, Reported by ACI Committee, vol. 544.

[50] G. Ramakrishna, T. Sundararajan, Impact strength of a few natural fibre reinforced cement mortar slabs: a comparative study, Cem. Concr. Compos. 27 (5) (2005) 547–553.

[51] A. Canakci, T. Varol, S. Ozsahin, Analysis of the effect of a new process control agent technique on the mechanical milling process using a neural network model: measurement and modeling, Measurement 46 (6) (2013) 1818–1827.

[52] Y. Cao, E. Kamrani, S. Mirzaei, A. Khandakar, B. Vaferi, Electrical efficiency of the photovoltaic/thermal collectors cooled by nanofluids: machine learning simulation and optimization by evolutionary algorithm, Energy Rep. 8 (2022) 24–36.

[53] B. Vaferi, R. Eslamloueyan, S. Ayatollahi, Automatic recognition of oil reservoir models from well testing data by using multi-layer perceptron networks, J. Pet. Sci. Eng. 77 (3-4) (2011) 254–262.

[54] A.T. Nair, A.R. Makwana, M.M. Ahammed, The use of response surface methodology for modelling and analysis of water and wastewater treatment processes: a review, Water Sci. Technol. 69 (3) (2014) 464–478.

[55] M.A. Hadiyat, B.M. Sopha, B.S. Wibowo, Response surface methodology using observational data: a systematic literature review, Appl. Sci. 12 (20) (2022) 10663.

[56] R. Abousnina, et al., Mechanical properties of macro polypropylene fibre-reinforced concrete, Polymers 13 (23) (2021) 4112. ⟨https://www.mdpi.com/2073-4360/13/23/4112⟩ ([Online]. Available).

[57] J. Ahmad, F. Aslam, R. Martínez-García, J. de Prado-Gil, N. Abbas, E.I. Hechmi, M. Ouni, Mechanical performance of concrete reinforced with polypropylene fibers (PPFs), J. Eng. Fibers Fabr. 16 (2021), p. 15589250211060399.

[58] D. Deti, M.W. Tjaronge, M.A. Caronge, Compressive loading and response time behavior of concrete containing refractory brick coarse aggregates, J. Eng. Appl. Sci. 71 (1) (2024) 95, https://doi.org/10.1186/s44147-024-00433-7.

[59] American Concrete Institute, Farmington Hills, MI, 2013.

[60] M.K. Yew, et al., Influences of macro polypropylene fibre-reinforced lightweight concrete incorporating recycled crushed LECA aggregate (Year), in: IOP Conference Series: Materials Science and Engineering, 1117, IOP Publishing, 2021 012009 (Year).

[61] D. Altalabani, D.K. Bzeni, S. Linsel, Mechanical properties and load deflection relationship of polypropylene fiber reinforced self-compacting lightweight concrete, Constr. Build. Mater. 252 (2020) 119084.

[62] I.A. Ja'e, et al., Optimisation of mechanical properties and impact resistance of basalt fibre reinforced concrete containing silica fume: Experimental and response surface assessment, Dev. Built Environ. 17 (2024) 100368, https://doi.org/10.1016/j.dibe.2024.100368.

[63] Lakshmi, A., Pandit, P., Bhagwat, Y., and Nayak, G.,(2022) A review on efficiency of polypropylene fiber-reinforced concrete, *Sustainability Trends and Challenges in Civil Engineering: Select Proceedings of CTCS 2020,* pp. 799-812.

[64] I.A. Ja'e, et al., Experimental and predictive evaluation of mechanical properties of kenaf-polypropylene fibre-reinforced concrete using response surface methodology, Dev. Built Environ. 16 (2023) 100262, https://doi.org/10.1016/j.dibe.2023.100262.

[65] R.Z. Al-Rousan, M.A. Alhassan, H. Al-Salman, Impact resistance of polypropylene fiber reinforced concrete two-way slabs, Struct. Eng. Mech. 62 (3) (2017) 373–380.

[66] D.-Y. Yoo, Y.-S. Yoon, Influence of steel fibers and fiber-reinforced polymers on the impact resistance of one-way concrete slabs, J. Compos. Mater. 48 (6) (2014) 695–706.

[67] J. Karthik, H. Surendra, V. Prathibha, G.A. Kumar, Experimental study on lightweight concrete using Leca, silica fume, and limestone as aggregates, Mater. Today.: Proc. 66 (2022) 2478–2482.

[68] N. Liang, S. Geng, J. Mao, X. Liu, X. Zhou, Investigation on cracking resistance mechanism of basalt-polypropylene fiber reinforced concrete based on SEM test, Constr. Build. Mater. 411 (2024) 134102, https://doi.org/10.1016/j.conbuildmat.2023.134102.

[69] D. Shen, X. Liu, X. Zeng, X. Zhao, G. Jiang, Effect of polypropylene plastic fibers length on cracking resistance of high performance concrete at early age, Constr. Build. Mater. 244 (2020) 117874, https://doi.org/10.1016/j.conbuildmat.2019.117874.